FABRICATION AND CHARACTERIZATION OF POLYCARBONATE SUBSTRATES FOR HIGH YIELD ASSEMBLY OF MULTICOMPONENT BIOHYBRID MICROROBOTS

Taryn Imamura, Utku M. Sonmez, Matthew Travers, Sarah Bergbreiter, Rebecca E. Taylor
Carnegie Mellon University, Pittsburgh, Pennsylvania, USA

ABSTRACT

This paper presents polycarbonate negative topographies used as substrates for the templated self-assembly of microsphere-based microrobots. This approach protects primary structures from damage during molding and de-molding, providing high fidelity negatives of arrays for assembly via templated assembly by selective removal (TASR). We show that reducing the surface energy mismatch between the microspheres and substrate results in yield increases up to 790%. This work addresses yield-related challenges of multicomponent microsystem assembly with existing PDMS-based templated assembly methods. The application of this technology in DNA microswimmer fabrication is demonstrated.

KEYWORDS

Self-assembly, Polycarbonate Heat (PCH) Molding, Templated Assembly by Selective Removal (TASR), Two-Photon Polymerization (TPP), Microswimmer

INTRODUCTION

Complex multicomponent microrobots, such as microswimmers, have potential applications in electronics, microfluidic mixing, and targeted drug delivery [1-2]. To realize the potential of this technology, fabrication methods must be capable of making large, monodisperse populations of robots. One example of a process to fabricate microswimmers is a hybrid top-down/bottom-up manufacturing process that combines templated assembly by selective removal (TASR) with DNA nanotechnology [3]. In this process, hydrophobic interactions drive the deposition of polystyrene microspheres into size-matched, hemispherical pockets constructed from Polydimethylsiloxane (PDMS). Sonication removes improperly matched particles and DNA nanotubes connect the spheres via biotin-streptavidin binding [3]. Previously, microsphere-based robots were made from random arrangements of particles assembled via one-pot reactions or magnetic manipulation [4-5]. TASR improves on these methods by controlling both the size and placement of components during fabrication, resulting in precise assembly of complex, multi-component structures.

However, yields of this process were exceptionally low, resulting in single digit populations of 2-bead microswimmers. For multicomponent systems, yield decreases with increasing complexity [6]. To build complex multicomponent structures, high yields are required at each stage of manufacturing. Therefore, the complexity and yield of recent multicomponent microrobots made via TASR has been limited. To improve this process, we considered the fundamental principles behind TASR: (1) microsphere pocketing is dependent on the interplay between surface energy and kinetic energy [7] and (2) contact area between microspheres and pockets is also necessary for assembly [8]. Because the TASR-based microswimmer process was not optimized for these parameters, we identified an opportunity to increase yield by addressing that gap.

In this paper, we leverage polycarbonate heat (PCH) molding to create TASR molds for assembling polystyrene beads, enabling high yield production of multi-component microswimmers. We hypothesize that material choice will improve yield through better surface energy matching to polystyrene components and that our two-photon polymerization (TPP) and multistep molding process can replicate hemispherical features with high fidelity. This approach additionally protects the primary structure from damage during molding and de-molding, reducing the cost and increasing robustness of the self-assembly process. Here we quantitatively confirm the fidelity our process to ensure sufficient microsphere contact area. We also studied the impact of surface energy on microsphere assembly by comparing pocketing yields for PDMS and PC substrates. Finally, we applied PCH molded substrates to TASR-based microswimmer fabrication, demonstrating multifold improvements in yield of 2-bead microassemblies, and the creation of a locomoting biohybrid DNA microswimmer.

FABRICATION

To assemble polystyrene microspheres for microswimmer production, TASR assembly sites must be compatible with microsphere shape and surface energies. To create pocketing geometries shape-matched to

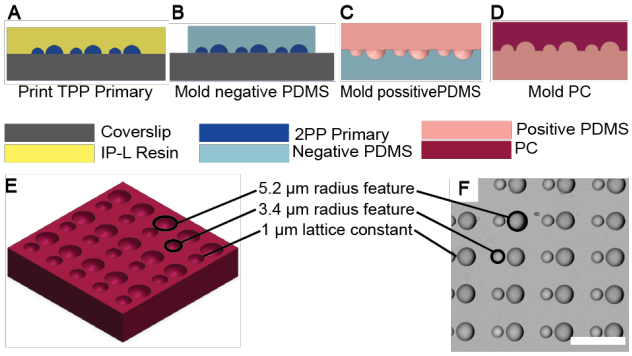

Figure 1: The fabrication process of the polycarbonate (PC) microstructure assembly substrates. (A) Desired structures are printed on a glass substrate using two-photon polymerization (TPP). (B) Negative molds are made in PDMS. (C) Positive copies of features are molded from PDMS. (D) PC is slowly baked over the positive PDMS features to create a topography of assembly sites. (E) Fabricated sites are 5.3 µm and 3.2 µm in radius. (F) An SEM image of the fabricated structures from top-down view. Scale bar is 30 µm.

microspheres, we developed a process that combines TPP with subsequent elastomer and PCH molding (Fig.1). Secondary molding steps provide the flexibility to fabricate geometries in materials other than elastomers or printable resins. TPP can print structures with resolution as low as 100 nm, ideal for making assembly sites precisely shape-matched to microsphere components [9].

To make the TPP primary mold (Fig. 1A), an array of 1024 paired hemispheres with radii of 5.2 µm and 3.4 µm was designed in SolidWorks. This array was printed directly on a No. 1.5 glass coverslip with a Nanoscribe Photonic Professional GT + (Nanoscribe Gmbh) using oil immersion mode and a negative photoresist (IP-L, Nanoscribe). A 63x/NA1.4 objective lens (Zeiss) with a laser power of 40 mW and a scanning speed 10,000 µm/s was used. The hatching distance was 0.02 µm and the hatching angle was 0° with a 60° offset. The slicing distance was varied from 0.5 µm to 1 µm to reduce surface roughness, thus maximizing contact area between molded pockets and the microsphere. The TPP primary mold was developed in propylene glycol methyl ether acetate (PGMEA, Sigma-Aldrich) for 20 min, then immersed in Isopropyl Alcohol (IPA, VWR) for 2 min to wash away any remaining developer and photoresist.

To reduce adhesion and aid in de-molding, the coverslip was incubated at room temperature for 12 hours in 10 mL Ethanol (VWR) with 100 µL silane (Trichloro(1H,1H,2H,2H-perfluorooctyl) silane, Sigma-Aldrich). To create the PDMS negative (Fig. 1B) a thin layer of PDMS (Sylgard 184, Dow Corning) was degassed and baked over the substrate at 70°C for 4 hours. The negative PDMS mold was then placed in a vacuum chamber with 3 drops of silane, which was evaporated under vacuum and allowed to settle over the negative PDMS mold for 12 hours, forming a layer to aid in de-molding. The positive PDMS mold (Fig. 1C) was made by pouring degassed PDMS over the silanized negative PDMS mold, creating a PDMS copy of the TPP primary mold.

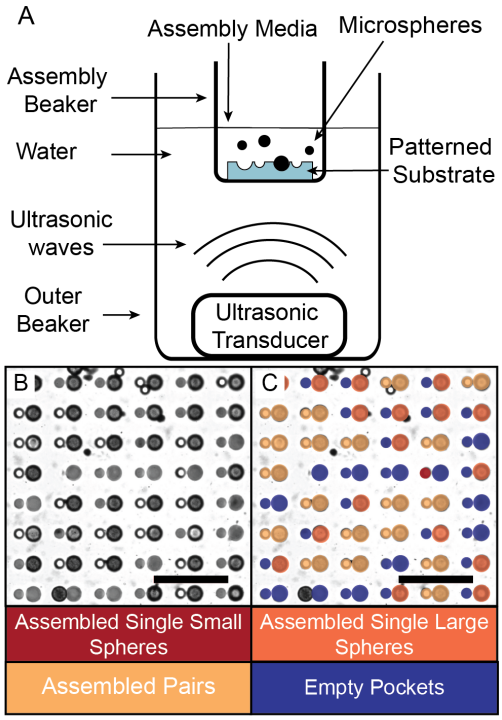

Figure 2: (A) The experimental setup for characterizing the microsphere assembly capabilities of the fabricated substrate. (B) Two sizes of microspheres are assembled in the PC TASR substrate. (C) Individual and parallel pocketing events are identified as shown by the colored mask provided. Scale bars are 50 µm.

The positive PDMS was coated with silane by the same process, then dried in a convection oven at 80°C for 14 hours to prevent air bubbles during PCH molding. Adapting protocols by Sonmez et al. [10], a PC sheet was also dehydrated at 120° C for 24 hours before molding to prevent the formation of bubbles. Immediately after drying, the PC disc was placed on top of the positive PDMS mold (Fig. 1D), and the assembly was baked in a vacuum oven under 508 mmHg at 230° C for 6 hours. The system was momentarily returned to atmospheric pressure twice during the molding process to mitigate air bubble formation, and the vacuum was released for the last hour of the bake. The PC disc was allowed to resolidify at room temperature for two hours. The positive PDMS molds were removed, and the PC TASR arrays were cut using a bandsaw and rotary tool. This process resulted in identical negative molds for TASR assembly made from both PDMS and PC.

EXPERIMENTAL SETUP

To test our process's ability to generate arrays capable of multi-bead assembly, we leveraged the TASR microrobot approach by Harmatz et al. [3]. PDMS and PC TASR templates were placed in a 10 mL assembly beaker and submerged in 8% aqueous ethanol until the substrate was covered by approximately 1 cm of solution. A 1000 mL beaker was filled with 600 mL of water, and a probe sonicator (Advanced Sonics) attached to a variable voltage transducer (Variac) was submerged in the center of the beaker. The assembly beaker was lowered into the large beaker until their liquid levels were even (Fig. 2A). Streptavidin-coated ferromagnetic and polystyrene microspheres (Spherotech Inc.) were deposited onto the substrate, given one minute to settle, and sonicated for removal (Fig. 2B). This process is repeated for each microsphere population. The spheres had average diameters respectively of 10.4 µm (SD of 0.60 µm) and 6.9 µm (SD of 1.17 µm) and were suspended in 1xTAE 12.5 mM $MgCl_2$ at concentrations of 0.5% weight/volume. Assembled spheres were viewed and counted using differential interference contrast (DIC) imaging on an upright microscope (Nikon), and categorized as: single 6.9 µm diameter spheres, single 10.4 µm diameter spheres, or assembled sphere pairs (Fig. 2C).

RESULTS

PCH molding has previously demonstrated high fidelity replication of microfeature dimensions [10]. However, because TASR yields depend on pocket shape, quantification of hemisphere dimensions at each step shown in Fig. 1 was essential to confirm the fidelity of feature transfer. To capture substrate features with high resolution, a benchtop SEM (Nanoscience Phenom XL) was used to collect images. Features were translucent and likely to charge during imaging, so samples were sputtered with 10 nm Au (EMS Q300T D Plus) to aid in the

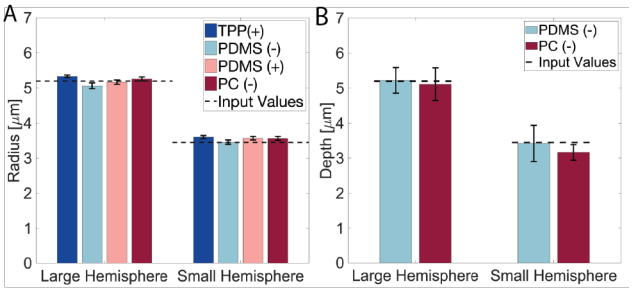

Figure 3: Radii and depth measurements for the small and large features for each step of the fabrication process.

collection of high-quality images. ImageJ Analyze Circle was used to identify circular features and report their radii.

Feature radii averages remained relatively constant at each step and had low standard deviations (Fig. 3A). Radius irregularity was observed amongst features from the four substrates, particularly for the negative PDMS. However, positive and negative features may bias image-based measurements resulting in the apparent reduction in radius for the negative PDMS mold. The average hemisphere radii were 5.1 µm and 3.3 µm for the negative PDMS, 5.3 µm and 3.4 µm for PC. Compared to the input design, this produces a percent error of less than 3.5% for each substrate and feature.

To evaluate the features aspect ratios, the maximum pocket depth for the negative PDMS and PC substrates were measured using a confocal microscope (Zeiss LSM 800). Confocal microscopy is useful for measuring features at this scale that are difficult to assess using stylus profilometry. For feature aspect ratios to be correct, pocket depths would need to be approximately 5.2 µm and 3.4 µm. The average depths for the negative PDMS substrate were 5.2 µm and 3.4 µm, while the average depths for the PC substrate were 5.1 µm and 3.1 µm. Compared to the nominal design, error was less than 2% for the large hemisphere and less than 10% for the small hemisphere for both substrates (Fig. 3B). The higher standard deviation most likely resulted from noise in the confocal images. Based on the consistency of feature radius and depth after each mold, we concluded that features were successfully transferred from PDMS to PC.

To show that our fabrication approach could assemble heterogenous components in parallel, microspheres were assembled in the PC substrate. The assembly rates for individuals and pairs were recorded (Fig. 4A). For each of 5 trials, the rate of assembly for adjacent microsphere pairs was lower than for individual components, demonstrating that higher yields are needed as microstructure complexity increases. Notably, there was sizable variation between trials even under consistent experimental conditions.

To characterize how surface energy impacts TASR assembly, the pocketing yields for PC were compared to the PDMS standard. The hydrophobicity of materials can be measured using the contact angle between a drop of water and the substrate surface. The contact angle of polystyrene, PDMS, and PC have been recorded as 85°, >100°, and 85° - 90° respectively [11]–[13]. We hypothesized that the PC substrate will exhibit higher yields because PC and polystyrene have a smaller difference in surface energies.

To test this hypothesis, assembly of microsphere pairs was assessed for a range of ultrasonic transducer voltages ranging from 40 V to 100 V. This sweep was repeated 3 times for each substrate. At higher voltages, the mean pocketing event counts for PC were substantially higher than for PDMS (Fig. 4B). For the 90V condition, the PC substrate provided a parallel assembly yield increase of 790% compared to the PDMS, supporting our hypothesis that better surface energy matching would lead to increased pocketing yields for multicomponent systems. Despite the large variability, the impact of sonication voltage on pocketing yield was found to be statistically significant using a Friedman's Test at 5% significance ($p = 0.03$). The largest average yield occurred at 90V, therefore this condition for TASR was adopted for all further microswimmer production.

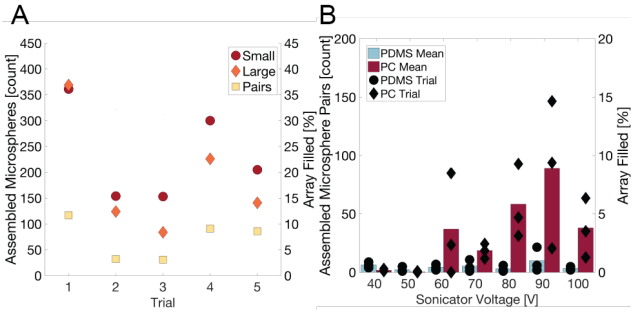

Figure 4: (A) Paired assembly of heterogeneous microspheres occurred at lower rates than individuals. (B) Microsphere assembly yields for the PC substrate far exceeded yields for the PDMS standard.

The ultimate aim of this technology is to fabricate complex, multicomponent microrobots via self-assembly. To demonstrate our technology's use for this application, DNA microswimmers were made using the PC substrate. Adjacently-pocketed microsphere pairs were attached using 10-helix DNA nanotubes. The DNA nanotubes were made by annealing 40 component oligomer strands and were suspended in 1XTAE with 12.5mM $MgCl_2$ at a concertation of 1 µM [14]. The nanotubes were biotinylated to facilitate binding with the streptavidin-coated microspheres. To connect adjacently-assembled beads, 321 pocketed microsphere pairs were incubated in the nanotube solution at 22°C for 2 hours.

Improved surface energy matching also increased the difficulty of depocketing microspheres. Therefore a gentle depocketing approach was developed using partially-cured PDMS, which was pressed against filled substrates and gently peeled to remove the microspheres from the assembly substrate. This method effectively removed multi-sphere assemblies while maintaining their structure and modifications. Thereafter, microswimmers were magnetically pulled from the PDMS into a solution of Percoll (Sigma-Aldrich) and 14 µm diameter polystyrene microsphere "fiducial markers" (Spherotech Inc.). The resulting microswimmers consisted of two rigid links, one ferromagnetic microsphere from the 5.2 µm radius pocket and one polystyrene microsphere size-matched to the 3.4 µm radius pocket, connected by a deformable link composed of DNA nanotubes (Fig. 5).

The microswimmers were deposited in a microfluidic channel for observation via brightfield microscopy and were actuated using a pair of orthogonal Helmholtz coils.

The magnetic field vector oscillated sinusoidally, causing the magnetic sphere to oscillate relative to the polystyrene sphere. The trajectories of the microswimmers and nonmagnetic fiducial spheres were tracked using TEMA, a tracking software for unmarked particles. Resulting two-bead microswimmers locomoted with an average velocity of 2.1 μm/s (Fig. 5), and future studies will investigate microswimmer dynamics and control.

CONCLUSONS

In this work, we have developed a manufacturing method for the realization of increasingly complex, multicomponent microrobots. This fabrication process utilizes TASR templates and leverages both TPP with PCH molding. High fidelity replication of micron-scale features were quantitatively confirmed and parallel assembly of heterogeneous polystyrene microspheres was demonstrated. Using PC TASR substrates, yield increases of up to 790% were observed, supporting our hypothesis that surface energy matching between microspheres and substrates would improve yields. Using PC TASR substrates resulted in multifold improvements for 2-bead microassembly yields, and the production of locomoting biohybrid DNA microswimmers. These findings directly address the complexity and yield limitations of existing templated assembly methods for multicomponent microrobots. In future studies, larger arrays and more intricate TASR patterning can be used to further increase yields and produce more complex structures, facilitating the study of multicomponent microrobots.

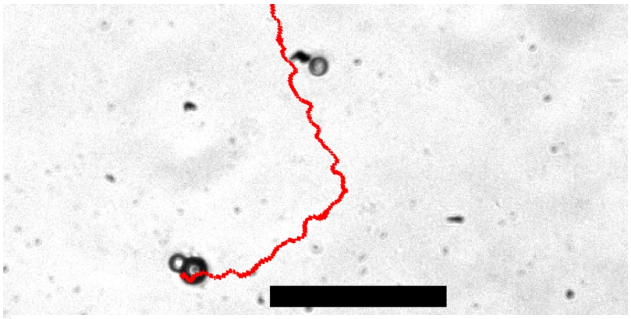

Figure 5: Locomoting 2-bead microswimmer created via templated assembly with PC. Scale bar is 70 μm.

ACKNOWLEDGEMENTS

This work was supported in part by the National Science Foundation (NSF) grants 1739308 and 2132886 and an NSF GRFP DGE1745016/DGE2140739. The authors would like to thank the staff of the Soft Lithography Lab at Carnegie Mellon University. Special thanks are given to Sukjun Kim for his expertise and training in TPP and to Jiya Janowitz for his support.

REFERENCES

[1] C. Hu, S. Pané, and B. J. Nelson, "Annual Review of Control, Robotics, and Autonomous Systems Soft Micro-and Nanorobotics," *Annu. Rev. Control Robot. Auton. Syst. 2018*, vol. 1, pp. 53–75, 2018, doi: 10.1146/annurev-control-060117.

[2] K. E. Peyer, L. Zhang, and B. J. Nelson, "Bio-inspired magnetic swimming microrobots for biomedical applications," *Nanoscale*, vol. 5, no. 4, pp. 1259–1272, 2013, doi: 10.1039/c2nr32554c.

[3] I. M. Harmatz, M. J. Travers, and R. E. Taylor, "A Customizable DNA and Microsphere-Based, Magnetically Actuated Microswimmer," *J. Microelectromechanical Syst.*, vol. 29, no. 5, pp. 990–995, 2020, doi: 10.1109/JMEMS.2020.3011610.

[4] P. Tierno, R. Golestanian, I. Pagonabarraga, and F. Sagués, "Controlled Swimming in Confined Fluids of Magnetically Actuated Colloidal Rotors," 2008, doi: 10.1103/PhysRevLett.101.218304.

[5] U. K. Cheang and M. J. Kim, "Self-assembly of robotic micro-and nanoswimmers using magnetic nanoparticles," doi: 10.1007/s11051-014-2737-z.

[6] G. Tikhomirov, P. Petersen, and L. Qian, "Fractal assembly of micrometre-scale DNA origami arrays with arbitrary patterns," *Nature*, vol. 552, no. 7683, pp. 67–71, 2017, doi: 10.1038/nature24655.

[7] S. Jung, F. Eid, and C. Livermore, "Modeling and characterizing initial component assembly in templated assembly by selective removal," *IEEE Trans. Nanotechnol.*, vol. 11, no. 1, pp. 152–159, 2012, doi: 10.1109/TNANO.2011.2164094.

[8] S. Jung and C. Livermore, "Achieving selective assembly with template topography and ultrasonically induced fluid forces," *Nano Lett.*, vol. 5, no. 11, pp. 2188–2194, 2005, doi: 10.1021/nl051221b.

[9] C. N. LaFratta, J. T. Fourkas, T. Baldacchini, and R. A. Farrer, "Multiphoton Fabrication," *Angew. Chemie Int. Ed.*, vol. 46, no. 33, pp. 6238–6258, Aug. 2007, doi: 10.1002/ANIE.200603995.

[10] U. M. Sonmez, S. Coyle, R. E. Taylor, and P. R. LeDuc, "Polycarbonate Heat Molding for Soft Lithography," *Small*, vol. 16, no. 16, pp. 1–12, 2020, doi: 10.1002/smll.202000241.

[11] E. Thormann, A. C. Simonsen, P. L. Hansen, and O. G. Mouritsen, "Interactions between a polystyrene particle and hydrophilic and hydrophobic surfaces in aqueous solutions," *Langmuir*, vol. 24, no. 14, pp. 7278–7284, Jul. 2008, doi: 10.1021/la8005162.

[12] Y. A. Alzahid *et al.*, "Functionalisation of Polydimethylsiloxane (PDMS)-Microfluidic Devices coated with Rock Minerals OPEN," doi: 10.1038/s41598-018-33495-8.

[13] P. Jankowski, D. Ogonczyk, A. Kosinski, W. Lisowski, and P. Garstecki, "Hydrophobic modification of polycarbonate for reproducible and stable formation of biocompatible microparticles," doi: 10.1039/c0lc00360c.

[14] P. Yin *et al.*, "Programming DNA tube circumferences," *Science (80-.).*, vol. 321, no. 5890, pp. 824–826, 2008, doi: 10.1126/science.1157312.

CONTACT

*T. Imamura, tri@andrew.cmu.edu